FACTA UNIVERSITATIS
Series: **Electronics and Energetics** Vol. 37, Nº 3, September 2024, pp. 497 – 516
https://doi.org/10.2298/FUEE2403497K

Original scientific paper

ENHANCING THE LVRT CAPABILITY OF GRID CONNECTED PV SYSTEM UNDER DISTURBED CONDITIONS USING A NOVEL APPROACH

Aakriti Khanna[1], Anjali Garg[2], Shradha Singh Parihar[3]

[1,2]The NorthCap University, Gurugram, India,
[3] Greater Noida Institute of Technology, Greater Noida, India

ORCID iDs:	Aakriti Khanna	https://orcid.org/0000-0003-2792-3473
	Anjali Garg	https://orcid.org/0000-0001-8157-0379
	Shradha Singh Parihar	https://orcid.org/0000-0001-8809-4504

Abstract. *Nowadays, the occurrence of low voltages or voltage sags is a common challenge during the operation of a three-phase grid-connected photovoltaic (PV) system. This research paper proposes an innovative approach to enhance the low voltage ride-through (LVRT) capability of such systems. The novel strategy proposed here relies on the concept of eliciting active components (EAC) which involves injecting active power during voltage sags, generating reference currents to operate the voltage source inverter and additionally incorporating an active component algorithm for maximizing the power point tracking from the PV array. The system considered for simulation considers a PV module with a maximum power of 382.9 W. The faults considered for the discussion are Line-Line-Line (LLL), Line-Line (LL), Line-Line-Ground (LLG) and Line-Ground (LG) faults. The approach also considers low grid voltage and frequent grid voltage fluctuation. The efficiency of this novel control method is evaluated in terms of fault clearance time and is further compared to the traditional controllers in compliance with the Indian grid code LVRT requirements. The obtained results indicate that this approach significantly reduces fault clearance time by 69.6% and 20.08% for LLG fault & 88.8% and 72% for LG fault in comparison to SRFT and SOGI control strategy, respectively. It also enhances DC link voltage stability in comparison to conventional control strategies during low voltage conditions. The approach ensures that the photovoltaic system remains connected without interruption during fault periods.*

Key words: *Photovoltaic, DC link voltage, LVRT, voltage sags, active power*

Received April 14, 2024; revised May 21, 2024 and June 06, 2024; accepted June 11, 2024
Corresponding author: Aakriti Khanna
The NorthCap University, Gurugram, India
E-mail: aaki.0502@gmail.com

1. INTRODUCTION

1.1. Motivation

The inexpensive and clean nature of the sun has gained attention of the researchers and power developers. For electric power generation, the photovoltaic (PV) industry is the strongest pillar. To meet the ever-increasing demand for power, solar power plants are extensively used with the grid [1-3]. While grid-connected PV systems hold vast potential for renewable energy generation, they often encounter a substantial number of grid faults. These faults, arising from various factors, present challenges to the seamless integration and reliability of the photovoltaic infrastructure within the grid. One of the critical grid faults is the voltage sag. Hence, it becomes obligatory to overcome this low voltage condition for a grid connected PV system, failing which causes system failure.

1.2. Literature Survey

Every country designs/revises the standard grid codes keeping in mind the fault ride through capabilities [4]. The Low voltage ride through (LVRT) capability intimates the dedication of the power generating source to remain in connection with the grid during and after the fault (voltage sag) occurs [5-7]. The importance of LVRT in PV inverters to maintain grid connection during short-term disturbances has been discussed in [8]. This paper delves into control strategies to address challenges during LVRT, emphasizing the significance of grid stability in PV systems. In [9], voltage sag generator (VSG) has been used to explore the impact of renewable energy systems on power quality and stability to focus on LVRT regulations for medium to high voltage applications without considering different grid disturbances.

The research in [10] involves experimental validation of various LVRT strategies using actual PV installations. It provides insights into the practical challenges and performance of LVRT strategies under real grid conditions. But, the study focuses on specific case studies and may not generalize across different grid environments and PV system configurations. Various studies have been performed by the researchers for the grid faults and for the improvement in the LVRT strategies. Proportional integral controller based voltage control has been implemented using the salp swarm algorithm (SSA) in [11], the technique has less ability to adapt to frequent changes. Synchronous reference frame-phase locked loop (SRF-PLL) technique has been presented for the control of inverter [12] but, this is inefficient for disturbed grid conditions such as frequent grid voltage fluctuations. Super capacitors are used at the DC side to absorb the unused power resulting in the avoidance of fluctuations in DC voltage, thereby; improving LVRT but the strategy increased the cost [13]. In [14], a neuro-fuzzy control system was implemented to manage voltage and power in a grid-connected photovoltaic (PV) system. This method improves sensitivity, but it results in a highly complex design that necessitates extensive training. In [14], a neuro-fuzzy control system was implemented to manage voltage and power in a grid-connected photovoltaic (PV) system. This method improves sensitivity, but it results in a highly complex design that necessitates extensive training.

Different controllers have been designed for LVRT capability, a few of which are droop controller, PQ controller, sliding controller, dq controller with PI and fuzzy [15-19], etc. Instantaneous active reactive control (IARC) has been discussed in [20] which uses the positive sequence (PS) and negative sequence (NS) voltages with acceptable total harmonic

distortion (THD) in normal operation; however, the technique results in high THD under sag condition. The second order generalized integrator (SOGI) is effective at detecting grid voltage sags with high robustness and quick dynamic response. However, it falls short in terms of simplicity of implementation [21]. Three-level neutral-point clamped (3L-NPC) inverters have been utilized for low voltage ride through (LVRT) as shown in [22]. These techniques involve complex filtering processes, leading to significant computational time for fault clearance, and primarily rely on reactive power injection. The marine predator algorithm, as discussed in [23], has been applied to LVRT conditions, focusing on the tuning of proportional-integral (PI) controllers for inverter control. However, its application is limited to three-phase short circuit (LLLG) fault conditions.

1.3. Paper Contributions

It has been seen from the existing literature survey, that the low voltage condition is a major source of system failure. Hence, the proposed control strategy for the three phase grid connected PV system deals with riding through such conditions. In this article, different types of faults are considered for the evaluation. Below are outlined the major contributions of this research paper:

1) A novel control strategy based on eliciting active components (EAC) has been developed for the first time which involves injecting active power during low voltage conditions and hence eliminates the reactive power injection and usage of complex filters.
2) The strategy has been tested for different complexities considering: Line-Line-Line (LLL), Line-Line (LL), Line-Line-Ground (LLG), Line-Ground (LG), low grid voltage and frequent grid voltage fluctuation.
3) The results attained for three phase disturbed grid using the EAC strategy have been further compared with the other techniques to validate the proposed technique and is found to be beneficial for the polluted grids.
4) The results ensure the safety of components preventing the disconnection of PV during the fault occurrence with the elimination of zero crossing detector and sample-hold circuitry.

1.4. Paper Organization

This paper is organized in the given flow: Section 2 provides LVRT requirement as per Indian grid code; Section 3 explains the system description with details of modelling the PV array and grid connected PV system. Section 4 presents the strategies considered for the analysis. Section 5 implements the proposed control strategy and analyzes the results obtained. Section 6 compares the results obtained using conventional strategies and the proposed strategy. Section 7 concludes the paper with its future scope.

2. LVRT Requirement in reference to Indian grid code

The Central Electricity Authority (CEA) of India sets the technical standards [20] for connectivity of the renewable energy sources to the grid. As per CEA, LVRT capability is must for the smooth operation of grid connected systems. LVRT requirement for PV penetration as per Indian Grid Code (IGC) is shown in Fig. 1, which presents the variation

in grid voltage (Vg) w.r.t time. Fig. 1 clearly shows that to avoid power loss in the system, the connectivity of PV system with the grid is mandatory even if the voltage drops below its working value. The voltage profile also shows that the connected PV system must provide the reactive power to the grid till 300ms or till the recovery stage is reached, whichever is acquired first. This is required to keep the voltage source inverter operational and to keep the system stable.

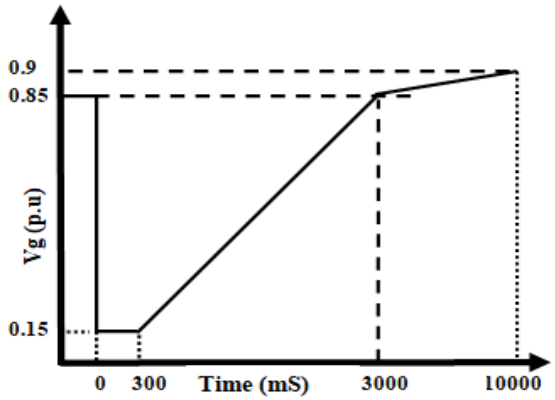

Fig. 1 LVRT requirement as per Indian Grid Code [24]

According to IGC, reactive current (I_q) and active current (I_d) injected during the LVRT period are given by (1) and (2) respectively and as mentioned below.

$$I_q = \begin{cases} 0\ (\text{deadband}) & 0.85\text{pu} \le V_g \le 1.1\text{pu} \\ K_a * (1 - V_g) * I_n & 0.50\text{pu} \le V_g \le 0.85\text{pu} \\ I_n & V_g < 0.50pu \end{cases} \quad (1)$$

$$I_d = \begin{cases} I_n & 0.85\text{pu} \le V_g \le 1.1\text{pu} \\ \sqrt{I_n^2 - I_q^2} & 0.50\text{pu} \le V_g \le 0.85\text{pu} \\ 0 & V_g < 0.50pu \end{cases} \quad (2)$$

where, I_n is the rated grid current , K_a is adjustment factor ($K_a \ge 2$) and Vg is grid voltage in pu.

3. System Description

The modeling of the system has been discussed and explained in the following subsections.

3.1. Modeling of PV system

PV model can be represented by a single diode model [25] or a two diode model. Equivalent circuit of PV model formed using a single diode is presented in Fig. 2 [26].

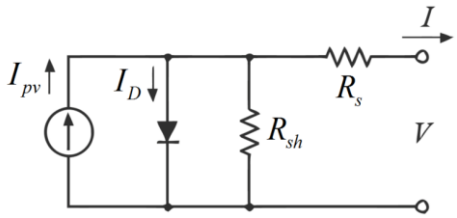

Fig. 2 Equivalent circuit of single diode PV model [26]

where, R_s is series resistance, R_{sh} is shunt resistance, I_D is diode current, Ipv is photocurrent. The PV module output current is obtained using characteristic equation (3).

$$I = Ipv - Is\left(\exp\frac{q(V+RsI)}{NKT} - 1\right) - \frac{V+RsI}{Rsh} \quad (3)$$

The parameters used in the characteristic equation are Boltzmann constant (K), reverse saturation current (Is), electron charge (q), series connected cells (N) and operating temperature (T). The PV module characteristics are illustrated in Fig.3.

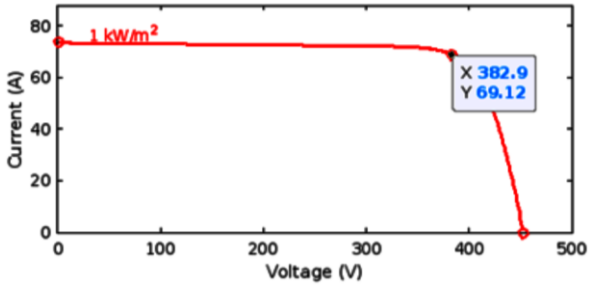

(a) I-V characteristic

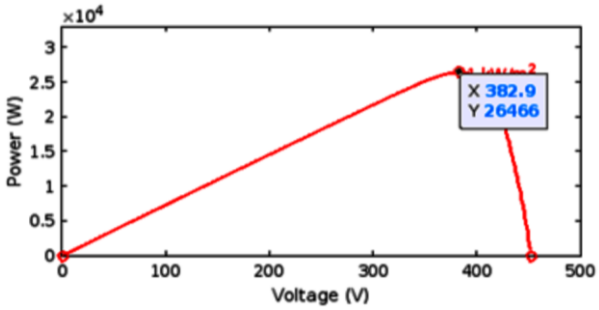

(b) P-V characteristic

Fig. 3 PV module characteristics

The parameters considered in the evaluation of the PV system are given in Table 1.

Table 1 PV system parameters

Symbol	Parameter	Value
P_{mpp}	Maximum power of Module	382.9 W
V_{mpp}	Maximum power point voltage of Module	54.7 V
V_{oc}	Open circuit voltage of Module	64.6 V
N	Number of cells per module	96
I_{mpp}	Maximum power point current of Module	5.76 A
R_s	Series resistance of model	389Ω
I_{sc}	Short circuit current of Module	6.14 A
N_p	Number of parallel strings in PV array	12
R_{sh}	Shunt resistance of model	0.33Ω
q	Electron charge	1.6×10^{-19}
N_s	Number of series modules per string in PV array	7
K	Boltzmann constant	1.38×10^{-23} JK^{-1}
T	Standard temperature	25ºC
I_r	Standard Solar Irradiance	1 kW/m^2

3.2. Modeling of Grid connected PV system

The modeling of grid connected PV system uses the components: PV array, DC-DC converter which is controlled by maximum power point tracking (MPPT) algorithm aiming at extracting maximum power from PV, DC-AC converter, AC grid and load connected at point of common coupling (PCC). The flow diagram illustrating the working is depicted in Fig.4.

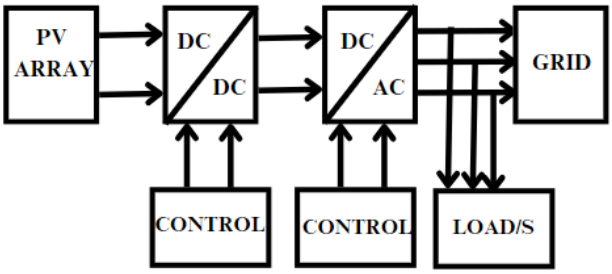

Fig. 4 Block diagram for working of grid connected PV system [27]

The ideal grid and DC link parameters considered in system modeling are tabulated in Table 2.

Table 2 Ideal Grid and DC link parameters [28]

Symbol	Parameter	Value
V_{rms}	Supply voltage	415 V
F_g	Frequency of ideal grid	50 Hz
C_{dc}	DC link capacitance	3000 µF

$V_{dc\ ref}$	DC link reference voltage	735 V

4. CONTROL STRATEGIES

In this paper, different control strategies have been applied to control the voltage source inverter (VSI) to work under various grid disturbances. The control strategies considered are mentioned below:

4.1. Traditional Control Strategies:

4.1.1. Synchronous reference frame theory (SRFT)

4.1.2. Second order generalized integrator (SOGI)

4.2. Proposed control strategy based on elicitation of active components (EAC)

4.1. Traditional Control Strategies

Traditional control strategies considered for the evaluation purpose are SRFT and SOGI as these have been widely used in the literature by the researchers due to their fast response and effective filtering. The traditional control strategies are explained below:

4.1.1. Synchronous reference frame theory

The SRFT control strategy is based on generation of reference currents by transformation between stationary and rotatory frames [29]. Fig. 5 presents the structure of SRFT. The proportional integral (PI) controller in SRFT is in-charge of adjusting the estimated frequency.

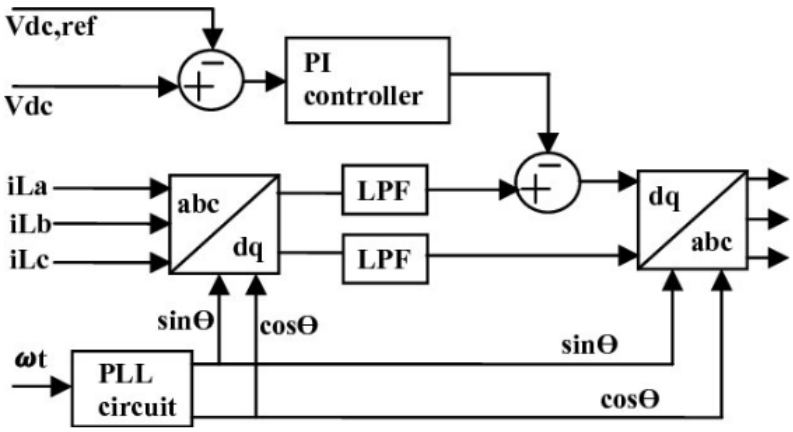

Fig. 5 Structure of SRFT [29]

4.1.2. Second order generalized integrator

The SOGI [30] technique is based on the generation of two orthogonal signals and works on frequency adaptive quadrature signal generation. The structure of SOGI shown in Fig.6 generates a pair of orthogonal signals v' and qv' which are sent for park transformation to obtain dq parameters. The phase error information contained in vq is

controlled to zero with the PI controller. The estimated phase angle Θ is then obtained using voltage controlled oscillator (VCO).

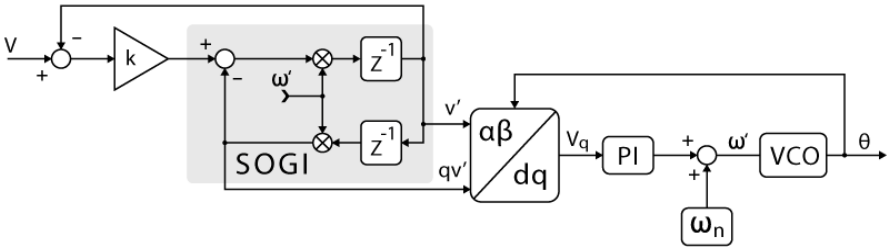

Fig. 6 Structure of SOGI [30]

4.2. Proposed control strategy based on elicitation of active components

The proposed control strategy has been presented for two modes of operation to validate the results of the control strategy, i.e.

i) Normal mode (with no voltage sag)
ii) LVRT mode

The working of the proposed strategy has been depicted in Fig. 7. The control strategy is based on elicitation of active components. The active current components are derived from the active segments of the unit templates (U_a, U_b and U_c). In the EAC approach, the line-to-line voltages (V_{ab} and V_{bc}) are measured and then used to determine the phase voltages. These phase voltages are subsequently converted into terminal voltage (V_{Gabc}). The phase voltage is essential for generating the unit template of each phase. The unit template is a reference waveform used in control algorithms to ensure that the inverter operates in synchronization with the grid. By accurately measuring and converting voltages at different stages, the system ensures precise control of the inverter, allowing it to inject the necessary active power to counteract voltage sags and maintain stable operation during faults. This meticulous process enhances the system's ability to ride through low voltage conditions effectively.

The unit templates and the load currents (I_{La}, I_{Lb} and I_{Lc}) of the three phases now elicit the respective active current component. In Fig.7, the three active current components ($i_{La}(e)$, $i_{Lb}(e)$, $i_{Lc}(e)$) contribute to the evaluation of total active current gain (I_{tacg}). Additionally, to maintain the stability of the DC link voltage, a comparison is conducted between the reference DC link voltage and the measured DC link voltage to find the DC link current gain (i_D). The two gains i.e. DC link current gain and total active current gain result in the formulation of the reference current gain (I_R).

The unit templates are then multiplied with the reference current gains to calculate the reference grid currents for each phase. Following this, the reference grid currents are compared with the actual grid currents to generate gate pulses which are required for the proper functioning of VSI for both modes of operation.

The EAC strategy has minimum mathematical blocks, which give a high advantage to the implementation of the control strategy ensuring minimum oscillations. The strategy handles the disturbances by injecting the active power in the grid.

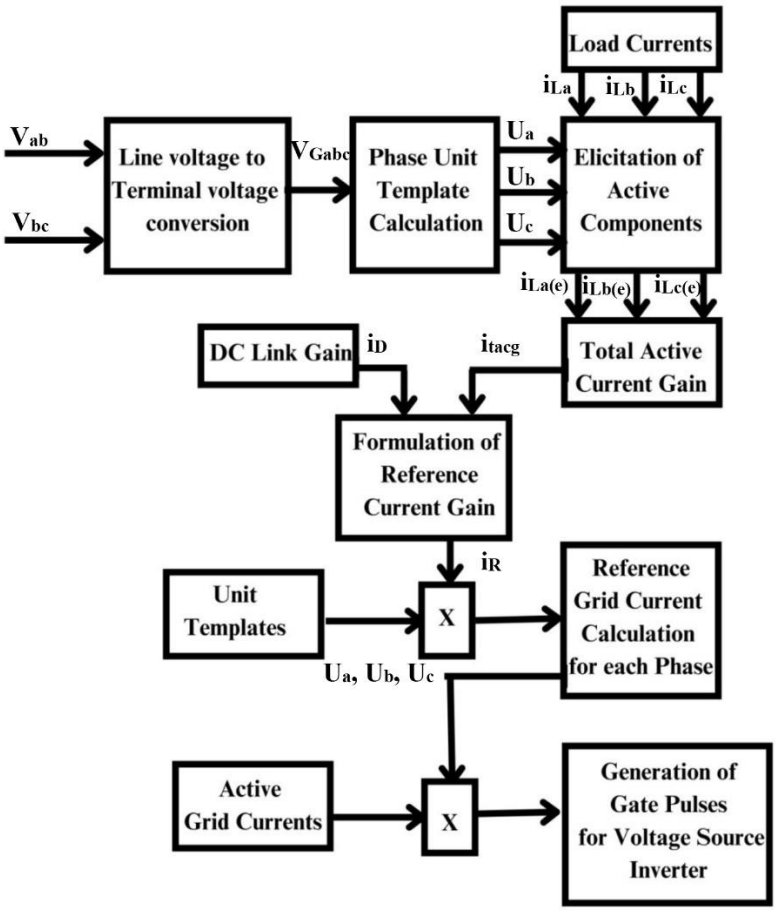

Fig. 7 Block diagram of the proposed control strategy - EAC

The unit template for each phase is obtained using (4)-(6).

$$U_a = \frac{V_{Ga}}{V_G} \tag{4}$$

$$U_b = \frac{V_{Gb}}{V_G} \tag{5}$$

$$U_c = \frac{V_{Gc}}{V_G} \tag{6}$$

where, v_{Ga}, v_{Gb} and v_{Gc} are the amplitude of respective phase voltages at PCC. The amplitude of the voltage at PCC (v_G) can be obtained using (7).

$$v_G = \sqrt{\frac{2}{3}\left(v_{Ga}^2 + v_{Gb}^2 + v_{Gc}^2\right)} \tag{7}$$

The elicitation of active current components for all phases is based on (8)-(10).

$$i_{La(e)} = \frac{\int_0^{wt}(i_{La}.u_a)d(wt)}{\int_0^{wt}(u_a.u_a)d(wt)} \quad (8)$$

$$i_{Lb(e)} = \frac{\int_0^{wt}(i_{Lb}.u_b)d(wt)}{\int_0^{wt}(u_b.u_b)d(wt)} \quad (9)$$

$$i_{Lc(e)} = \frac{\int_0^{wt}(i_{Lc}.u_c)d(wt)}{\int_0^{wt}(u_c.u_c)d(wt)} \quad (10)$$

The calculation of total active current gain is done using the average of individual active current components as in (11).

$$i_{tgac} = \frac{i_{La(e)}+i_{Lb(e)}+i_{Lc(e)}}{3} \quad (11)$$

The reference current gain is calculated using (12)

$$i_R = i_{tgac} + i_D \quad (12)$$

Reference grid currents are calculated by multiplication of (12) and unit templates for each phase ((4)-(6)).

5. IMPLEMENTATION & RESULTS

In this section, the performance evaluation of the proposed EAC strategy considering various types of faults has been carried out based on simulation results using MATLAB/Simulink tool. To enhance the LVRT capability, the EAC strategy has been employed for the system presented in Fig. 8(a). The detailed simulation of the proposed control strategy has been presented in Fig. 8(b).

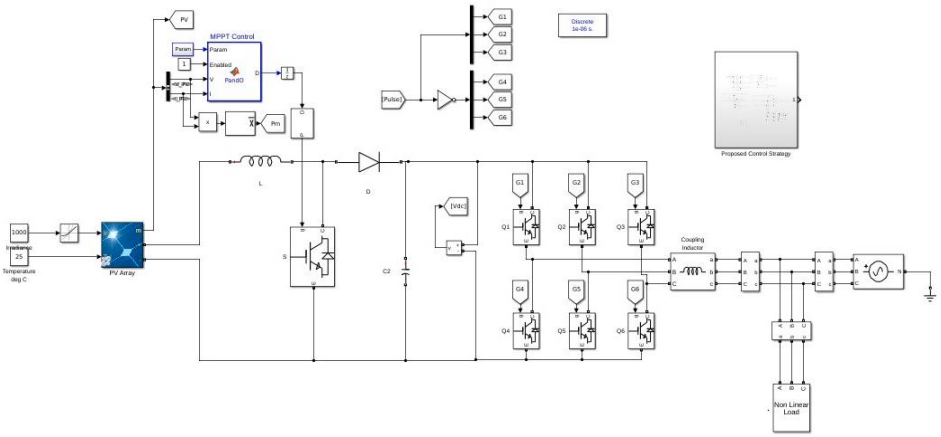

Fig. 8(a) EAC strategy based simulink model of three phase system

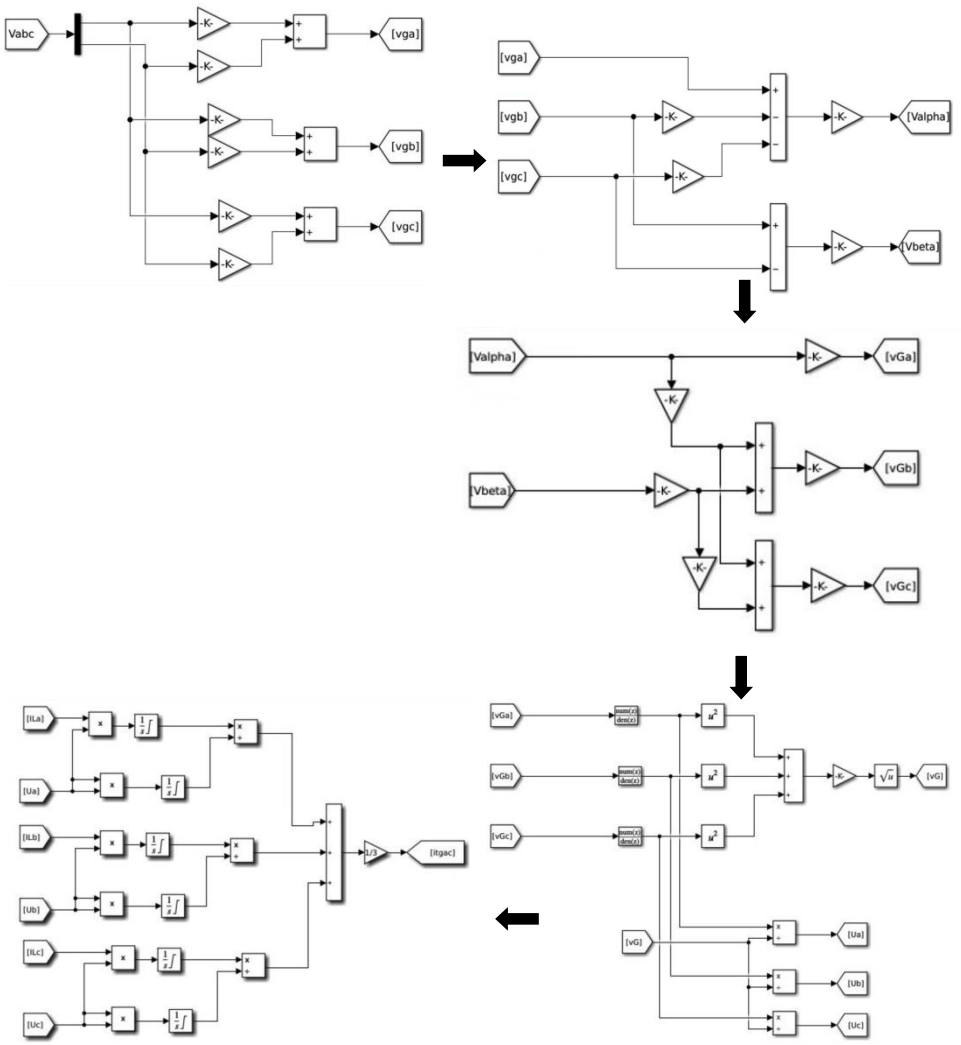

Fig. 8(b) Detailed simulation of proposed control strategy

Fig. 8 Simulation of the system using EAC control strategy

The evaluation results are simulated considering two different modes of operation:
(i) Normal Operation (with no voltage sag)
(ii) LVRT Operation

(i) Normal operation: The operation of grid connected system with no voltage sag/ no disturbance is known as the normal operation. The grid connected PV system is tested for standard test conditions (STC), i.e. 1000 W/m^2 and 25^{o}C. The system is also tested by varying the solar insolation of 700 W/m^2 to verify the working of the system designed under varying insolation conditions. Fig. 9 presents the output of the PV for the normal

mode of operation. The graphs in Fig. 9 presented for two solar irradiations are (a)solar irradiance (W/m^2), (b)PV voltage (V), (c)PV power (W), (d)grid voltage (V), grid current (A), (e)grid side active power P_{grid} (W), grid side reactive power Q_{grid} (VAR) and (f)DC link voltage V_{dc} (V) with respect to time (sec).

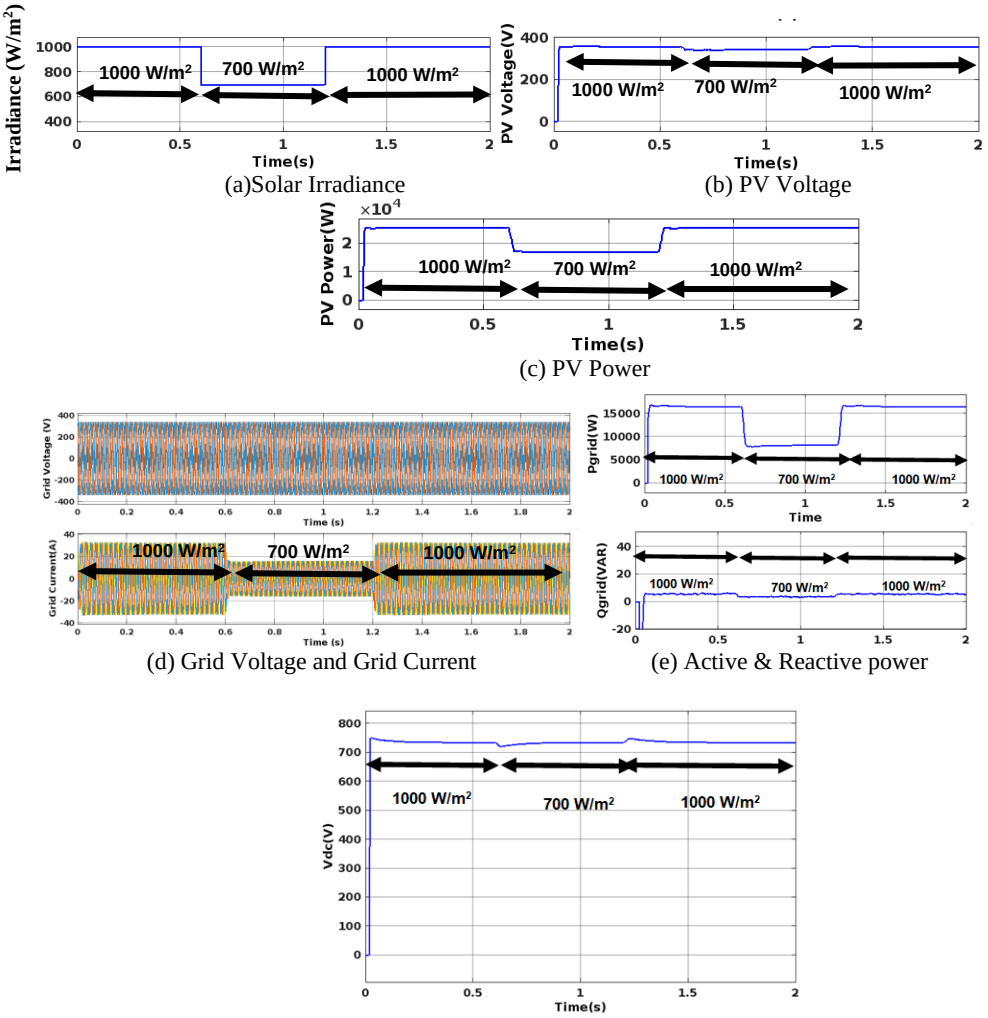

Fig. 9 PV system during normal mode of operation

It clearly infers that when there is no grid fault, the system operates optimally depending on the solar insolation captured by the PV source. The DC link voltage stability remains effectively preserved in absence of any grid faults.

(ii) LVRT operation: LVRT operation is the system operation when grid connected PV system undergoes grid disturbances. The disturbances considered for the evaluation are the following

faults: LLL, LL, LLG, LG, low grid voltage and frequent grid voltage fluctuation.

For LLL fault and LL fault: LLL fault is Line-Line-Line grid fault in which all the lines get short-circuited while LL fault is Line-Line grid fault in which two lines get short circuited. These faults mainly arise because of the breakdown of the insulation between the phases of the grid.

Fig. 10 shows the results which include grid voltage, grid current, active & reactive power of grid, DC link voltage plot using proposed EAC strategy for all the considered parameters. In this operation, STC are used for LLL fault which occurs for the time span 0.45s to 0.6s and LL fault which occurs from 1.3 s to 1.45 s.

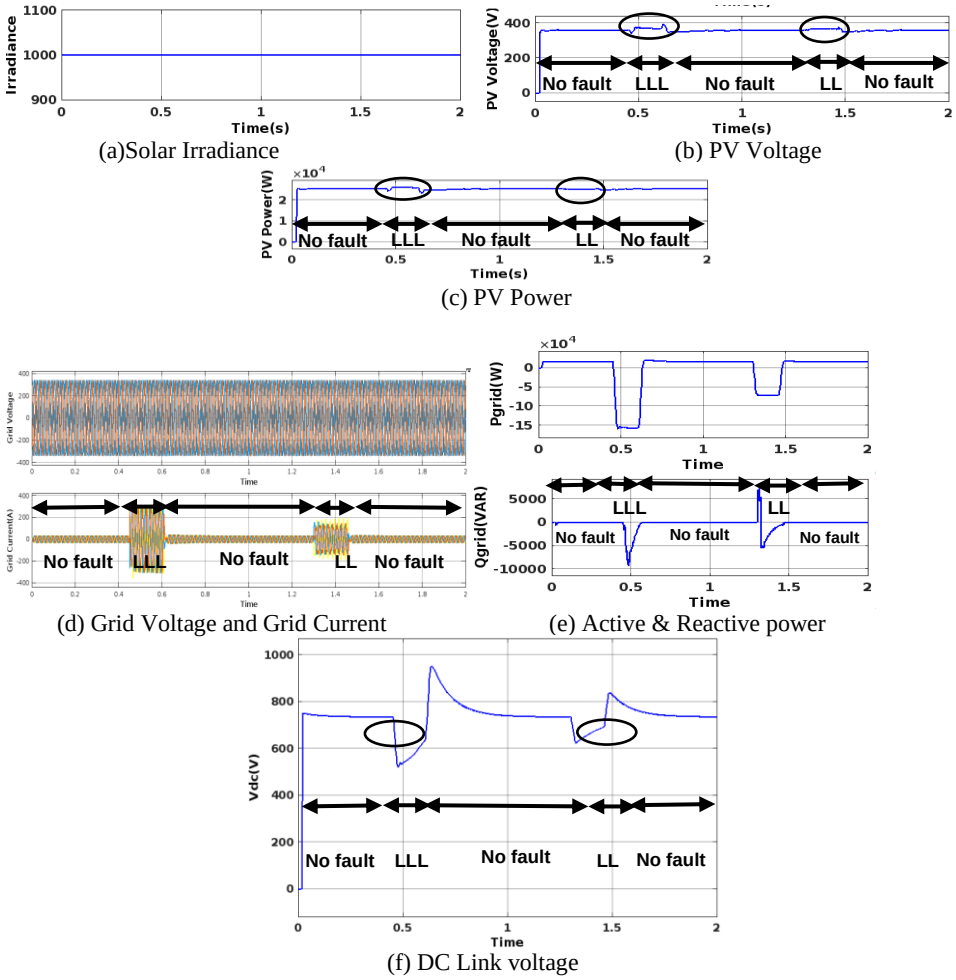

(a)Solar Irradiance (b) PV Voltage

(c) PV Power

(d) Grid Voltage and Grid Current (e) Active & Reactive power

(f) DC Link voltage

Fig. 10 EAC strategy based PV system during LLL and LL fault condition

The results presented in Fig. 10 depict that the simulated PV system remains in connection with the grid in reference to the IGC when the fault occurs. The restoration time is less than 225 ms which is less than acceptable time of 300 ms (as per IGC).

For LLG fault and LG fault: LLG fault is the Line-Line-Ground grid fault in which the two lines get short-circuited with earth while LG fault is the Line-Ground grid fault in which one of the lines gets short circuited with earth.

Fig. 11 demonstrates the results including the DC link voltage, PV voltage, power, active & reactive power of grid using the EAC strategy for the standard test conditions. Here, LLG fault occurs between 0.5s to 0.9s and LG fault occurs from 1.4s to 1.6 s.

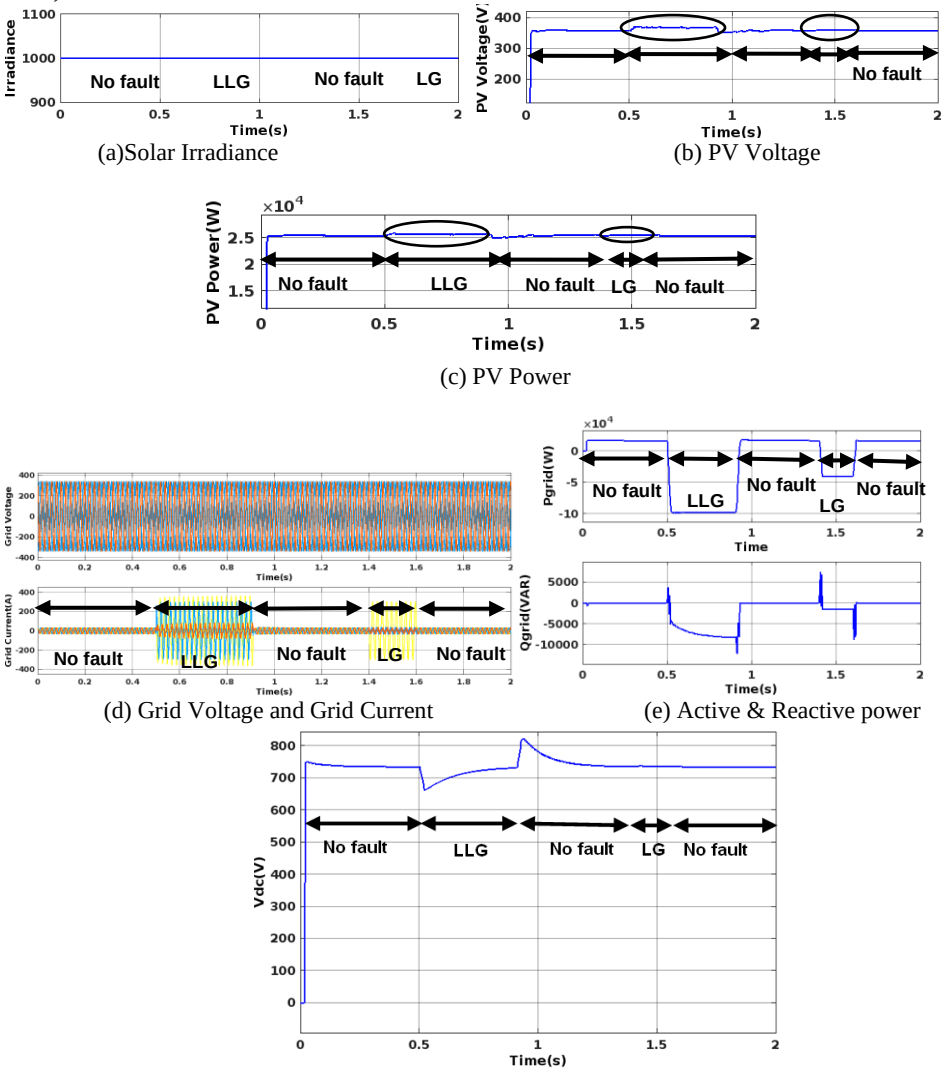

(a)Solar Irradiance (b) PV Voltage

(c) PV Power

(d) Grid Voltage and Grid Current (e) Active & Reactive power

(f) DC Link voltage

Fig. 11 EAC strategy based PV system during LLG and LG fault condition

As shown in Fig. 11, PV system remains connected and DC voltage stability is recovered within the permissible fault period of LLG and LG fault as per IGC.

For Low grid voltage: Low grid voltage is the condition of the dip in amplitude of grid voltage. Fig. 12 shows the PV system with proposed EAC strategy for standard test conditions with low grid voltage having amplitude 0.7pu for the time period 0.8s to 1.2s.

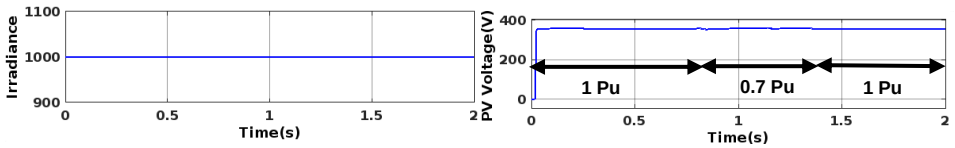

(a)Solar Irradiance (b) PV Voltage

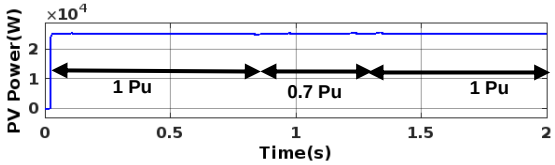

(c) PV Power

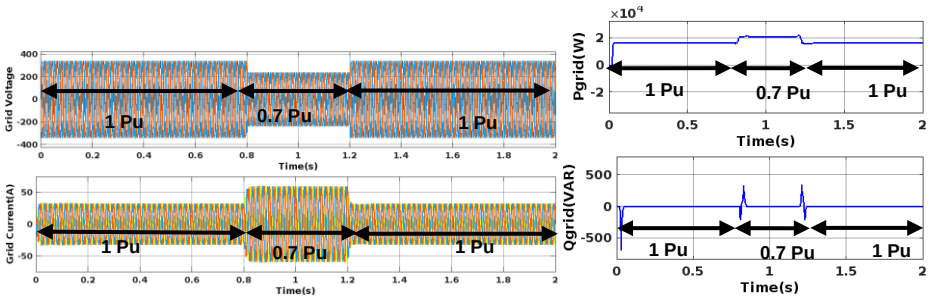

(d) Grid Voltage and Grid Current (e) Active & Reactive power

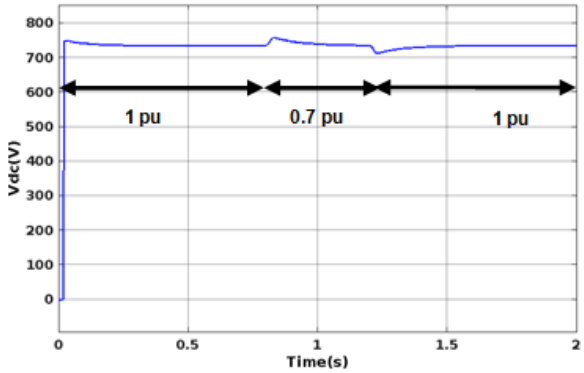

(f) DC Link voltage

Fig. 12 EAC strategy based PV system with 0.7 pu amplitude of grid voltage

From Fig. 12, it is evident that as the grid voltage decreases, the grid current rises. The proposed EAC in this case facilitates an increase in grid active power to maintain grid

stability, regulate DC link voltage and prevent PV disconnection. This strategy is crucial for sustaining grid stability.

For Frequent fluctuation in grid voltage with time: Here, the disturbance considered is frequent fluctuation in amplitude of grid voltage for the system under examination. Fig. 13 shows the system output for fluctuating values of grid voltages (1pu, 1.1pu, 0.6pu and 0.4pu) at different instants of time for standard test conditions.

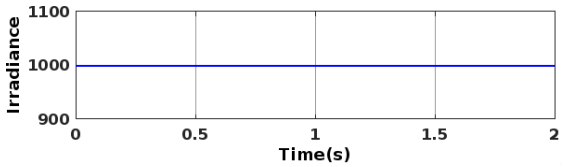

(a)Solar Irradiance

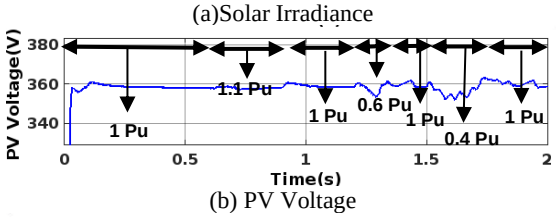

(b) PV Voltage

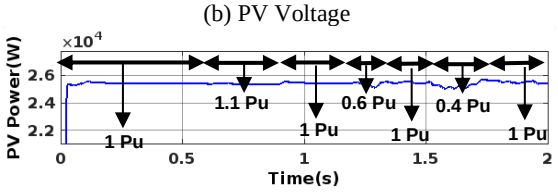

(c) PV Power

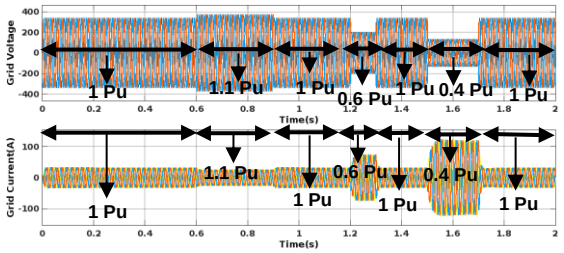

(d) Grid Voltage and Grid Current

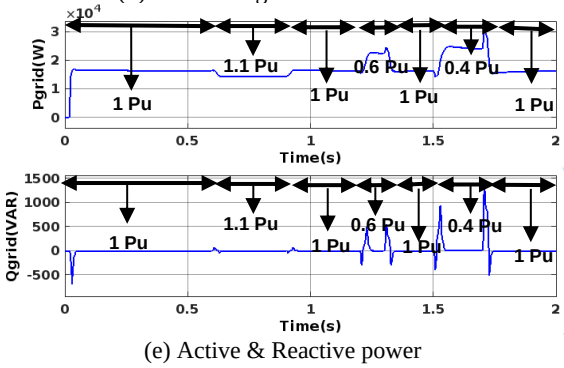

(e) Active & Reactive power

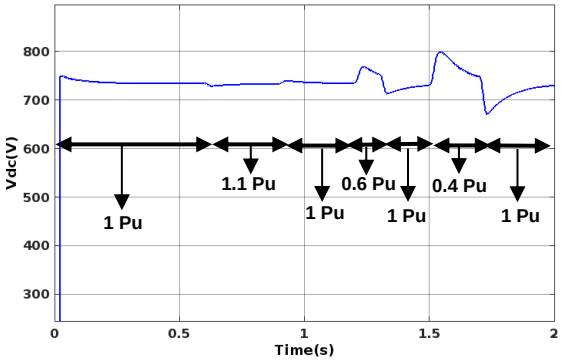

(f) DC Link voltage

Fig. 13 EAC strategy based PV system with fluctuating values of amplitude of grid voltage

Fig. 13 depicts the performance of the system employing EAC amidst voltage fluctuations. The system achieves stable DC voltage, effectively preventing PV disconnection during fault occurrences and ensuring reconnection within the specified timeframe outlined in the IGC.

6. Comparative Analysis Of Proposed Strategy with Traditional Methods

The proposed EAC control strategy is simulated on three phase system and compared based on time taken for the fault clearance with conventional strategies like SRFT [31] and SOGI [22,32]. The comparative analysis is tabulated in Table 3 for different fault scenarios.

Table 3 Comparative Analysis of proposed control strategy with the conventional control strategies based on fault clearance time

Type of disturbance		SRFT [31]	SOGI [22,32]	Proposed EAC	Percentage improvement w.r.t fault clearance time	
					EAC with SRFT[31]	EAC with SOGI[22,32]
Fault	LLL	625ms	225ms	215ms	65.6 %	4.44 %
	LL	625ms	265ms	225ms	64%	15.09%
	LLG	625ms	240ms	190ms	69.6 %	20.8%
	LG	625ms	250ms	70ms	88.8 %	72%
Frequent fluctuation of grid voltage	0.7 pu	-	-	200ms	-	-
	1.1 pu	-	-	210ms	-	-

From Table 3, it is clear that:

1) Fault clearance time taken by proposed EAC is very less in all the fault occurrence conditions.
2) For LLL fault: EAC takes 65.6% and 4.44% less % time as compared to SRFT and SOGI control strategies respectively.

3) For LL fault: EAC takes 64% and 15.09% less % time as compared to SRFT and SOGI respectively.
4) For LLG fault: the improvement in fault clearance time is 69.6% and 20.8% with SRFT and SOGI strategies respectively using EAC control strategy.
5) For LG fault: the % reduction in fault clearance is 88.8% and 72% for SRFT and SOGI respectively using EAC.
6) Additionally, the proposed EAC strategy effectively handles frequent fluctuations in amplitude of grid voltage.

7. CONCLUSION

This research paper proposed an innovative control approach, elicitation of active components, designed to uphold DC Link voltage and swiftly rectify faults during instances of low voltage in grid connected PV systems. The system's efficacy was evaluated across various fault scenarios: LLL, LL, LLG, LG, low grid voltage and frequent voltage fluctuations. The results indicate that the EAC approach promptly restores connection within the stipulated timeframes outlined in the IGC following a fault occurrence, showing a substantial % reduction in fault clearance time concerning conventional control strategies, thus ensuring uninterrupted grid connection.

The comparative analysis against conventional controllers, namely, SRFT and SOGI, revealed that the proposed strategy excels in both restoring DC link voltage and fault clearance time. The control strategy proposed in the paper shows maximum improvement in % reduction of fault clearance time in LG fault with 88.8% and 72% time reduction with respect to SRFT and SOGI control strategy respectively. The findings underscore the superior performance of the proposed approach in terms of improved stability and quick fault clearance time under various faulty conditions. The promising results achieved by the EAC control strategy open up several avenues for future research like real-time deployment and integration with hybrid renewable systems. Further, this work can also be extended for cost benefit analysis and different types of situations like varying solar insolations and frequency fluctuations.

REFERENCES

[1] G. Lammert, D. Premm, L.D.P. Ospina, J.C. Boemer, M. & T.V. Cutsem, "Control of photovoltaic systems for enhanced short-term voltage stability and recovery", *IEEE Trans. Energy Convers.*, vol. 34, pp. 243–254, 2019.
[2] B. Stojčetović, M. Petković, & S. Đurović, "Assessment of renewable energy sources using mcdm method: case study", *Facta Universitatis, Series: Electronics and Energetics*, vol. 36, no. 3, pp. 353–363, 2023.
[3] M. Preradovic, "Solar energy potential in Freiburg, Graz, Maribor, Banja Luka, Niš, and Athens", *Facta universitatis, Series: Electronics and Energetics*, vol. 35, no. 3, pp. 393–403, 2022.
[4] K. Zeb, S. U. Islam, I. Khan, W. Uddin, M. Ishfaq, T.D.C. Busarello, S.M. Muyeen, I.Ahmad & H.J. Kim, "Faults and Fault Ride Through strategies for grid-connected photovoltaic system: A comprehensive review", *Renewable and Sustainable Energy Reviews*, vol. 158, p. 112125, 2022.
[5] A. Marinopoulos, F. Papandrea, M. Reza, S. Norrga, F. Spertino, & R. Napoli, "Grid integration aspects of large solar PV installations: LVRT capability and reactive power/voltage support requirements", *IEEE Trondheim Power Tech, Trondheim, Norway*, pp. 1–8, 2011.
[6] E. Afshari, G.R. Moradi, R. Rahimi, B. Farhangi, Y.Yang, F. Blaabjerg, & S.Farhangi, "Control strategy for three-phase grid-connected PV inverters enabling current limitation under unbalanced faults", *IEEE Trans. Ind. Electron.*, vol. 64, no. 11, pp. 8908–8918, 2017.

[7] M.A. Khan, A. Haque, & V.S.B. Kurukuru, "Dynamic voltage support for low-voltage ride-through operation in single-phase grid-connected photovoltaic systems", *IEEE Transactions on Power Electronics*, vol. 36, no. 10, pp. 12102–12111, 2021.
[8] J. Joshi, A.K. Swami, V. Jately, & B. Azzopardi, "A comprehensive review of control strategies to overcome challenges during LVRT in PV systems", *IEEE Access*, vol. 9, pp. 121804–121834, 2021.
[9] Y. Yang, F. Blaabjerg, & Z. Zou, "Benchmarking of voltage sag generators", In Proceedings of the IECON 2012-38th Annual Conference on IEEE Industrial Electronics Society, 2012, pp. 943–948.
[10] J.P. Roselyn, C.P. Chandran, C. Nithya, D. Devaraj, R. Venkatesan, V. Gopal, & S. Madhura, "Design and implementation of fuzzy logic based modified real-reactive power control of inverter for low voltage ride through enhancement in grid connected solar PV system", *Control Engineering Practice*, vol. 101, 2020.
[11] O.S. Elazab, M. Debouza, H.M. Hasanien, S.M. Muyeen, & A. Al-Durra, "Salp swarm algorithm-based optimal control scheme for LVRT capability improvement of grid-connected photovoltaic power plants: Design and experimental validation", *IET Renew. Power Gener.*, vol. 14, no. 4, pp. 591–599, 2020.
[12] S. Bagchi, D. Chatterjee, R. Bhaduri, & P.K. Biswas, "An alternative inverter control strategy for grid connected solar photovoltaic (SPV) system", In Proceedings of the IEEE 9th Power India International Conference (PIICON), Sonepat, 2020, pp. 1–5.
[13] H. Tian, F. Gao, & C. Ma, "Novel low voltage ride through strategy of single-stage grid-tied photovoltaic inverter with super capacitor coupled", In Proceedings of the Power Electronics and Motion Control Conf. IEEE (IPEMC), Harbin, China, 2012, vol. 2, pp. 1188–1192.
[14] F.-J. Lin, K.-C. Lu, T.-H. Ke, B.-H. Yang, & Y.-R. Chang, "Reactive power control of three-phase grid-connected PV system during grid faults using Takagi–Sugeno–Kang probabilistic fuzzy neural network control", *IEEE Trans. Ind. Electron.*, vol. 62, pp. 5516–5528, 2015.
[15] M.M. Hasaneen, M.A.L. Badr, & A.M. Atallah, "Control of active/reactive power and low-voltage ride through for 40 kW three-phase grid-connected single-stage PV system", In Proceedings of the 24th International Conference & Exhibition on Electricity Distribution (CIRED), 2017, pp.1655–1659.
[16] M.P. Petronijević, C. Milosavljević, B. Veselić, S. Huseinbegović, & B. Peruničić, "Discrete time quasi-sliding mode-based control of LCL grid inverters", *Facta Universitatis, Series: Electronics and Energetics*, vol. 36, no. 1, pp. 133–158, 2023.
[17] H.M. Hasanien, "An adaptive control strategy for Low Voltage Ride Through capability enhancement of grid-connected photovoltaic power plants". *IEEE Trans. Power Syst.*, vol. 31, no. 4, pp. 3230–3237, 2016.
[18] S. Mikkili, & A.K. Panda, "Instantaneous active and reactive power and current strategies for current harmonics cancellation in 3-ph 4-wire SHAF with both PI and fuzzy controllers", *Energy Power Eng.*, pp. 285–298, 2011.
[19] X. Zhao, J.M. Guerrero, M. Savaghebi, J.C. Vasquez, X.Wu, & K.Sun, "Low-voltage ride-through operation of power converters in grid interactive microgrids by using negative-sequence droop control", *IEEE Trans. Power Electron.*, vol. 32, no. 4, pp. 3128–3142, 2017.
[20] P. Rodriguez, A.V. Timbus, R. Teodorescu, M. Liserre, and F. Blaabjerg, "Flexible active power control of distributed power generation systems during grid faults", *IEEE Transactions on Industrial Electronics*, vol. 54, no. 5, pp. 2583–2592, 2007.
[21] J. Xu, H. Qian, Y. Hu, S. Bian, & S. Xie, "Overview of SOGI-based single-phase phase-locked loops for grid synchronization under complex grid conditions", *IEEE Access*, vol. 9, pp. 39275–39291, 2021.
[22] H.D. Tafti, A.I. Maswood, G. Konstantinou, J.Pou, K.Kandasamy, Z.Lim, & G.H.P. Ooi "Low-voltage ride-thorough capability of photovoltaic grid-connected neutral-point clamped inverters with active/reactive power injection", *IET Renew. Power Gener.*, vol. 11, no. 8, pp. 1182–1190, 2017.
[23] H.H. Ellithy, H.M. Hasanien, M. Alharbi, M.A. Sobhy, A.M. Taha, & M.A. Attia, "Marine Predator Algorithm-Based Optimal PI Controllers for LVRT Capability Enhancement of Grid-Connected PV Systems", *Biomimetics*, vol. 9, no. 2, 2024.
[24] Indian Grid code-CEA
[25] H.M. Ridha, H. Hizam, S. Mirjalili, M.L. Othman, M. E. Ya'acob, & L. Abualigah, "A Novel Theoretical and Practical Methodology for Extracting the Parameters of the Single and Double Diode Photovoltaic Models", *IEEE Access*, vol. 10, 2022.
[26] M.G. Villalva, J.R. Gazoli, & E.R. Filho, "Comprehensive approach to modeling and simulation of photovoltaic arrays", *IEEE Transactions on power electronics*, vol. 24, no. 5, pp. 1198–1208, 2009.
[27] A. Khanna, A. Garg, & S. Madichetty, "Harmonic Performance Analysis for Different Loads with and Without PV", In: Singhal, P., Kalra, S., Singh, B., Bansal, R.C. (eds) Recent Developments in Electrical and Electronics Engineering. Lecture Notes in Electrical Engineering, vol. 979. Springer, Singapore, 2023.
[28] J. Xu, H. Qian, S. Bian, Y. Hu, & S. Xie, "Comparative study of single-phase phase-locked loops for grid-connected inverters under non-ideal grid conditions", *CSEE Journal of Power and Energy Systems*, vol. 8, no. 1, pp. 155–164, 2020.

[29] P. Karuppanan, & K. Mahapatra, "A novel SRF based cascaded multilevel active filter for power line conditioners", In Proceedings of the 2010 Annual IEEE India Conference (INDICON), pp.1–4, 2010.
[30] A. Nagliero, R. A. Mastromauro, M. Liserre, & A. Dell'Aquila, "Monitoring and synchronization techniques for single-phase PV systems", In Proceedings of the SPEEDAM 2010, pp. 1404–1409.
[31] A.Q.Al-Shetwi, M.Z. Sujod, & F. Blaabjerg, "Low voltage ride-through capability control for Single-stage inverter-based grid-connected photovoltaic power plant", *Sol. Energy*, vol. 159, pp. 665–681, 2018.
[32] M. Talha, A. Amir, S.R.S. Raihan, & N.A. Rahim, "Grid-connected photovoltaic inverters with low-voltage ride through for a residential-scale system: A review", *International Transactions on Electrical Energy Systems*, vol. 31, no. 10, 2021.